Available online at www.sciencedirect.com

SciVerse ScienceDirect

Procedia Engineering 56 (2013) 54 – 62

Procedia Engineering

www.elsevier.com/locate/procedia

5th BSME International Conference on Thermal Engineering

Effect of Prandtl number on free convection in a solar collector filled with nanofluid

Rehena Nasrin*, Salma Parvin, M. A. Alim

Department of Mathematics, Bangladesh University of Engineering & Technology,Dhaka-1000, Bangladesh

Abstract

Numerical study of the influence of Prandtl number on free convection flow phenomena in a solar collector having glass cover plate and sinusoidal absorber is done. The working fluid is water-Al_2O_3 nanofluid. The cover plate has initially constant temperature T_h, while bottom absorber is at temperature T_c, with $T_h > T_c$. The remaining walls are considered adiabatic. By Penalty Finite Element Method the governing differential equations with boundary conditions are solved. The effect of the Prandtl number on the flow pattern and heat transfer has been depicted. Comprehensive average Nusselt number, average temperature and mean velocity inside the collector are presented as a function of the governing parameter mentioned above. The highest *Pr* causes the greatest heat transfer. The enhancing performance of heat transfer rate is more effective for the water-Al_2O_3 nanofluid than the base fluid.

Keywords: Water-Al_2O_3 nanofluid; solar collector; Prandtl number; finite element method.

1. Introduction

Because of the desirable environmental and safety aspects it is widely believed that solar energy should be utilized instead of other alternative energy forms, even when the costs involved are slightly higher. The flat-plate solar collector is commonly used today for the collection of low temperature solar thermal energy. Solar collectors are key elements in many applications, such as building heating systems, solar drying devices, etc. Solar energy has the greatest potential of all the sources of renewable energy especially when other sources in the country have depleted. The fluids with solid-sized nanoparticles suspended in them are called “nanofluids.” The natural convection in enclosures continues to be a very active area of research during the past few decades. Applications of nanoparticles in thermal field are to enhance heat transfer from solar collectors to storage tanks, to improve efficiency of coolants in transformers.

Conventional analysis and design of solar collector is based on a one-dimensional conduction equation formulation [1]. The analysis has been substantially assisted by the derivation of plate-fin efficiency factors. The factors relate the design and operating conditions of the collector in a systematic manner that facilitates prediction of heat collection rates at the design stage. The one-dimensional analysis offers a desired accuracy required in a routine analysis even though a two-dimensional temperature distribution exists over the absorber plate of the collector. Therefore, for more accurate analysis at low mass flow rates, a two-dimensional temperature distribution must be considered. Various investigators have used two dimensional conduction equations in their analysis with different boundary conditions.

* Corresponding author. Tel: +8801913583407
E-mail address: rehena@math.buet.ac.bd

doi:10.1016/j.proeng.2013.03.088

Nag et al. [2] used the two-dimensional model proposed by Lund, but with convection boundary condition at the upper and lower edge of the absorber plate. They solved the governing equations using finite element method. They concluded that the isotherms deviated from a one-dimensional pattern for a high flow rate to a predominantly two-dimensional distribution for a low mass flow rate. Stasiek [3] made experimental studies of heat transfer and fluid flow across corrugated and undulated heat exchanger surfaces. Piao et al. [4] investigated experimentally natural, forced and mixed convective heat transfer in a cross-corrugated channel solar air heater. Detailed experimental and numerical studies on the performance of the solar air heater were made by Gao [5].

There are so many methods introduced to increase the efficiency of the solar water heater [6–9]. But the novel approach is to introduce the nanofluids in solar water heater instead of conventional heat transfer fluids (like water). The poor heat transfer properties of these conventional fluids compared to most solids are the primary obstacle to the high compactness and effectiveness of the system. The essential initiative is to seek the solid particles having thermal conductivity of several hundred times higher than those of conventional fluids. These early studies, however, used suspensions of millimeter- or micrometer-sized particles, which, although showed some enhancement, experienced problems such as poor suspension stability and hence channel clogging, which are particularly serious for systems using mini sized and micro sized particles. The suspended metallic or nonmetallic nanoparticles change the transport properties and heat transfer characteristics of the base fluid. Stability and thermal conductivity characteristics of nanofluids was performed by Hwang et al. [10]. In this study, they concluded that the thermal conductivity of ethylene glycol was increased by 30%.

The absorptance of the collector surface for shortwave solar radiation depends on the nature and colour of the coating and on the incident angle. Usually black colour is used. Various colour coatings had been proposed in [11–13] mainly for aesthetic reasons. A low-cost mechanically manufactured selective solar absorber surface method had been proposed by Konttinen et al. [14]. These are usually low-cost units which can offer cost effective solar thermal energy in applications such as water preheating for domestic or industrial use, heating of swimming pools, space heating and air heating for industrial or agricultural applications. The principal requirement of the solar collector is a large contact area between the absorbing surface and the air.

In this paper, we investigate numerically the natural convection inside the solar collector having the flat-plate cover and wavelike absorber. The objective of this paper is to present flow and heat transfer used to harness solar energy.

Nomenclature

A_m	Dimensionless amplitude of wave
C_p	Specific heat at constant pressure (kJ kg^{-1} K^{-1})
g	Gravitational acceleration (m s^{-2})
h	Local heat transfer coefficient (W m^{-2} K^{-1})
k	Thermal conductivity (W m^{-1} K^{-1})
L	Length of the solar collector (m)
Nu	Nusselt number, $Nu = hL/k_f$
Pr	Prandtl number
Ra	Rayleigh number
T	Dimensional temperature (^{o}K)
T_i	Initial temperature of nanofluid (^{o}K)
u, v	Dimensional x and y components of velocity (m s^{-1})
U, V	Dimensionless velocities
X, Y	Dimensionless coordinates
x, y	Dimensional coordinates (m)

Greek Symbols

α	Fluid thermal diffusivity (m^2 s^{-1})
β	Thermal expansion coefficient (K^{-1})
ε	Emissivity
ϕ	Nanoparticles volume fraction
ν	Kinematic viscosity (m^2 s^{-1})
θ	Dimensionless temperature
ρ	Density (kg m^{-3})
λ	Number of wave
μ	Dynamic viscosity (N s m^{-2})

σ Stefan Boltzmann constant

ω Dimensionless velocity field

Subscripts

av average
c cold
f fluid
h hot
nf nanofluid
s solid particle
w top wall

2. Problem formulation

Figure 1 shows a schematic diagram of a solar collector. The fluid in the collector is water-based nanofluid containing Al_2O_3 nanoparticles. The nanofluid is assumed incompressible and the flow is considered to be laminar. It is taken that water and nanoparticles are in thermal equilibrium and no slip occurs between them. The solar collector is a metal box with a cover on top and a dark colored wavelike absorber plate on the bottom. The top horizontal wall has initially constant temperature T_h, while bottom sinusoidal wall is at temperature T_c, with $T_h > T_c$. The two vertical walls are considered adiabatic. The thermophysical properties of the nanofluid are taken from Lin and Violi [15] and given in Table 1. The density of the nanofluid is approximated by the Boussinesq model. Only steady state case is considered.

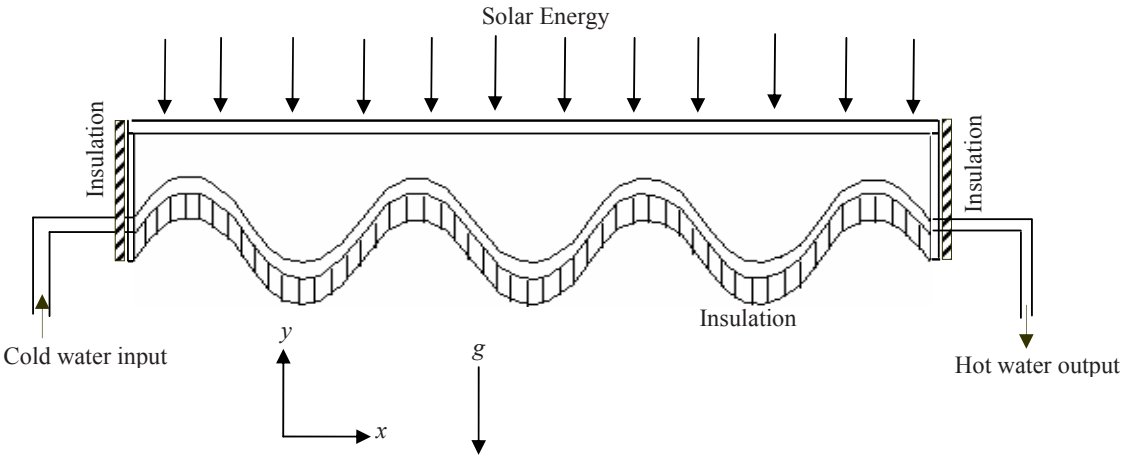

Fig.1. Schematic diagram of the solar collector

The governing equations for laminar natural convection in a solar collector filled with water-alumina nanofluid in terms of the Navier-Stokes and energy equation (dimensional form) are given as:
Continuity equation:

$$\frac{\partial u}{\partial x}+\frac{\partial v}{\partial y}=0 \qquad (1)$$

x-momentum equation:

$$\rho_{nf}\left(u\frac{\partial u}{\partial x}+v\frac{\partial u}{\partial y}\right)=-\frac{\partial p}{\partial x}+\mu_{nf}\left(\frac{\partial^2 u}{\partial x^2}+\frac{\partial^2 u}{\partial y^2}\right) \qquad (2)$$

y-momentum equation:

$$\rho_{nf}\left(u\frac{\partial v}{\partial x}+v\frac{\partial v}{\partial y}\right)=-\frac{\partial p}{\partial y}+\mu_{nf}\left(\frac{\partial^2 v}{\partial x^2}+\frac{\partial^2 v}{\partial y^2}\right)+g\rho_{nf}\beta_{nf}(T-T_c) \quad (3)$$

Energy equation:

$$u\frac{\partial T}{\partial x}+v\frac{\partial T}{\partial y}=\alpha_{nf}\left(\frac{\partial^2 T}{\partial x^2}+\frac{\partial^2 T}{\partial y^2}\right) \quad (4)$$

where, $\rho_{nf}=(1-\phi)\rho_f+\phi\rho_s$ is the density,

$(\rho C_p)_{nf}=(1-\phi)(\rho C_p)_f+\phi(\rho C_p)_s$ is the heat capacitance,

$\beta_{nf}=(1-\phi)\beta_f+\phi\beta_s$ is the thermal expansion coefficient,

$\alpha_{nf}=k_{nf}/(\rho C_p)_{nf}$ is the thermal diffusivity,

the dynamic viscosity of Brinkman model [16] is $\mu_{nf}=\mu_f(1-\phi)^{-2.5}$

and the thermal conductivity of Maxwell Garnett (MG) model [17] is $k_{nf}=k_f\dfrac{k_s+2k_f-2\phi(k_f-k_s)}{k_s+2k_f+\phi(k_f-k_s)}$.

Radiation heat transfer by the top glass cover surface must account for thermal radiation which can be absorbed, reflected, or transmitted. This decomposition can be expressed by,

$$q_{net}=q_{absorbed}+q_{transmitted}+q_{reflected}$$

Outside the boundary layer, the amount of energy $q_{reflected}$ is neglected.

Thus total energy of the glass cover plate becomes $q_{net}=q_{absorbed}+q_{transmitted}$

Now the amount of transmitted energy is radiated from the cover plate to the bottom wavy absorber without any medium as:

$$q_{transmitted}=q_r=\varepsilon\sigma A\left(T_w{}^4-T_c^4\right)$$

Here ε is emissivity of the glass cover plate, σ is Stefan Boltzmann constant 5.670400 x 10^{-8} $Js^{-1}m^{-2}K^{-4}$ and T_w is the variable temperature of the top wall. Again, the amount of absorbed energy is transferred from cover plate to bottom absorber by natural convection where medium is nanofluid as:

$$q_{absorbed}=q_c=hA(T_w-T_i)$$

So total energy gained or loosed by the cover plate is $q_{net}=hA(T_w-T_i)+\varepsilon\sigma A\left(T_w{}^4-T_c^4\right)$

The boundary conditions are:

at all solid boundaries $u = v = 0$

at the top cover plate $q=hA(T_w-T_i)+\varepsilon\sigma A\left(T_w{}^4-T_c^4\right)$

at the vertical walls $\dfrac{\partial T}{\partial x}=0$

at the bottom wavy absorber $T = T_c$

The above equations are non-dimensionalized by using the following dimensionless dependent and independent variables:

$$X=\frac{x}{L},\quad Y=\frac{y}{L},\quad U=\frac{uL}{\nu_f},\quad V=\frac{vL}{\nu_f},\quad P=\frac{pL^2}{\rho_f\nu_f{}^2},\theta=\frac{T-T_c}{T_h-T_c}$$

Then the non-dimensional governing equations are

$$\frac{\partial U}{\partial X}+\frac{\partial V}{\partial Y}=0 \quad (5)$$

$$U\frac{\partial U}{\partial X}+V\frac{\partial U}{\partial Y}=-\frac{\rho_f}{\rho_{nf}}\frac{\partial P}{\partial X}+Pr\frac{\nu_{nf}}{\nu_f}\left(\frac{\partial^2 U}{\partial X^2}+\frac{\partial^2 U}{\partial Y^2}\right) \quad (6)$$

$$U\frac{\partial V}{\partial X}+V\frac{\partial V}{\partial Y}=-\frac{\rho_f}{\rho_{nf}}\frac{\partial P}{\partial Y}+Pr\frac{\nu_{nf}}{\nu_f}\left(\frac{\partial^2 V}{\partial X^2}+\frac{\partial^2 V}{\partial Y^2}\right)+Ra\,Pr\frac{(1-\phi)\rho_f\beta_f+\phi\rho_s\beta_s}{\rho_{nf}\beta_f}\theta \quad (7)$$

$$U\frac{\partial \theta}{\partial X}+V\frac{\partial \theta}{\partial Y}=\frac{1}{Pr}\left(\frac{\partial^2 \theta}{\partial X^2}+\frac{\partial^2 \theta}{\partial Y^2}\right) \quad (8)$$

where $Pr=\frac{\nu_f}{\alpha_f}$ is the Prandtl number, $Ra=\frac{g\beta_f L^3\left(T_h-T_c\right)}{\nu_f^2}$ is the Rayleigh number.

The corresponding boundary conditions take the following form:
at all solid boundaries $U = V = 0$
at the vertical walls $\frac{\partial \theta}{\partial X}=0$
at the bottom wavy absorber $\theta = 0$

2.1. Average Nusselt number

The average Nusselt number (*Nu*) is expected to depend on a number of factors such as thermal conductivity, heat capacitance, viscosity, flow structure of nanofluids, volume fraction, dimensions and fractal distributions of nanoparticles.

The local variation of the convective Nusselt number of the fluid at the top cover plate is $\overline{Nu_c}=-\frac{k_{nf}}{k_f}\frac{\partial T}{\partial x}$.

The non-dimensional form of local convective heat transfer is $\overline{Nu}_c=-\frac{k_{nf}}{k_f}\frac{\partial \theta}{\partial X}$.

By integrating the local Nusselt number over the top heated surface, the average convective heat transfer along the heated wall of the collector is used by Saleh et al. [18] as $Nu_c=\int_0^1 \overline{Nu_c}\;dX$.

The radiated heat transfer rate is expressed as $Nu_r=\int_0^1 q_r\,dX$.

The average Nusselt number is $Nu = Nu_c + Nu_r$

The mean bulk temperature and average sub domain velocity of the fluid inside the collector may be written as $\theta_{av}=\int\theta\,d\overline{V}/\overline{V}$ and $\omega_{av}=\int\omega\,d\overline{V}/\overline{V}$, where $\overline{V}$ is the volume of the collector.

3. Numerical implementation

The Galerkin finite element method [19, 20] is used to solve the non-dimensional governing equations along with boundary conditions for the considered problem. The equation of continuity has been used as a constraint due to mass conservation and this restriction may be used to find the pressure distribution. The finite element method is used to solve the Eqs. (6) - (8), where the pressure *P* is eliminated by a constraint. The continuity equation is automatically fulfilled for large values of this constraint. Then the velocity components (*U*, *V*) and temperature (θ) are expanded using a basis set. The Galerkin finite element technique yields the subsequent nonlinear residual equations. Three points Gaussian quadrature is used to evaluate the integrals in these equations. The non-linear residual equations are solved using Newton–Raphson method to determine the coefficients of the expansions. The convergence of solutions is assumed when the relative error for each variable between consecutive iterations is recorded below the convergence criterion such that $\left|\psi^{n+1}-\psi^{n}\right|\le 10^{-4}$, where *n* is the number of iteration and Ψ is a function of *U*, *V* and θ.

3.1. Mesh Generation

In the finite element method, the mesh generation is the technique to subdivide a domain into a set of sub-domains, called finite elements, control volume, etc. The discrete locations are defined by the numerical grid, at which the variables

are to be calculated. It is basically a discrete representation of the geometric domain on which the problem is to be solved. The computational domains with irregular geometries by a collection of finite elements make the method a valuable practical tool for the solution of boundary value problems arising in various fields of engineering. Fig. 2 displays the finite element mesh of the present physical domain.

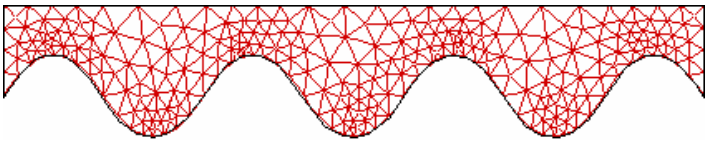

Fig. 2. Mesh generation of the collector

3.2. Grid independent test

An extensive mesh testing procedure is conducted to guarantee a grid-independent solution for $Ra = 10^4$and $Pr = 1.73$ in a solar collector. In the present work, we examine five different non-uniform grid systems with the following number of elements within the resolution field: 2969, 5130, 6916, 9057 and 11426. The numerical scheme is carried out for highly precise key in the average convective and radiated Nusselt numbers namely Nu_c and Nu_r for the aforesaid elements to develop an understanding of the grid fineness as shown in Table 2 and Fig. 3. The scale of the average Nusselt and Sherwood numbers for 9057 elements shows a little difference with the results obtained for the other elements. Hence, considering the non-uniform grid system of 9057 elements is preferred for the computation.

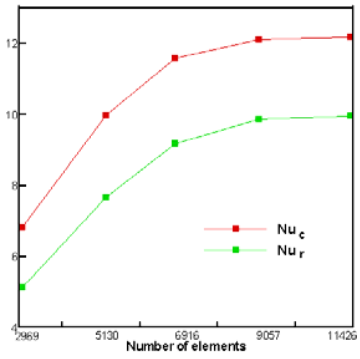

Fig. 3. Grid test for the geometry

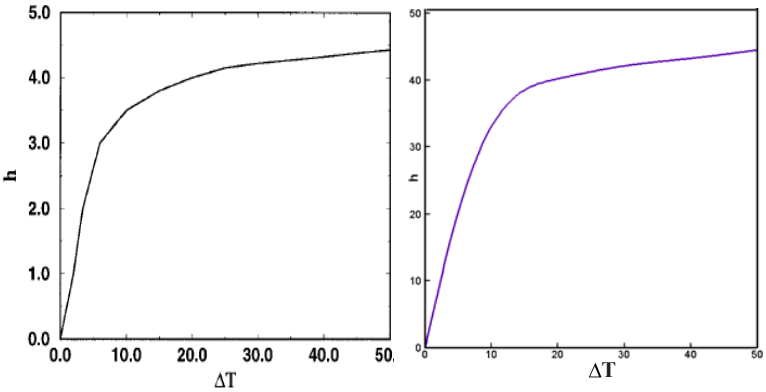

Gao et al. [21] Present Work

Fig. 4. Comparison of present code with Gao et al. [21] with $Pr = 0.73$ and $Ra = 10^4$

3.3. Code validation

The present numerical solution is validated by comparing the current code results for heat transfer - temperature difference profile at Pr = 0.73, $Gr = 10^4$ with the graphical representation of Gao et al. [21] which was reported for heat transfer augmentation inside a channel between the flat-plate cover and sine-wave absorber of a cross-corrugated solar air heater. Fig. 4 demonstrates the above stated comparison. As shown in Fig. 4, the numerical solutions (present work and Gao et al. [21]) are in good agreement.

4. Results and discussion

In this section, numerical results of streamlines and isotherms for various values of Prandtl number (Pr) with Al_2O_3 /water nanofluid in a solar collector are displayed. The considered values of Pr are Pr (= 1.73, 2.45, 3.77 and 6.62) while the Rayleigh number $Ra = 10^4$, the solid volume fraction ϕ = 5%, the emissivity ε = 0.9, the wave amplitude of bottom surface A_m = 0.075 and number of wave λ = 3.5. In addition, the values of the average Nusselt number both for convection and radiation as well as mean bulk temperature and average sub domain velocity profile are shown graphically.

Fig. 5 (a)–(b) exposes the heat transfer and fluid flow for various Prandtl number Pr (= 1.73-6.62). In this figure we observe that as the Prandtl number enhances from 1.73 to 6.62, the isothermal contours tend to get affected considerably. In addition, these lines corresponding to Pr = 6.62 become less bended whereas initially (Pr = 1.73) the lines take sinusoidal wavelike form. The isotherms cover the whole region of the solar collector due to comparatively higher temperature of the working water-Al_2O_3 nanofluid at the lowest Pr where the contour lines mimic the wall's (absorber) profile. Rising Prandtl number leads to deformation of the thermal boundary layer at the cold wavy absorber. However, the increase in the thermal gradients at the upper horizontal wall is much higher for the considered nanofluid than for the clear water. This means that higher heat transfer rate is predicted by the nanofluid than the base fluid (water). The fluid flow covers the entire collector at the lowest Pr forming few eddies. The streamlines have no significant change due to rising Pr except the core of the vortices becomes slightly smaller. This is expected because highly viscous fluid having larger Prandtl number does not move freely.

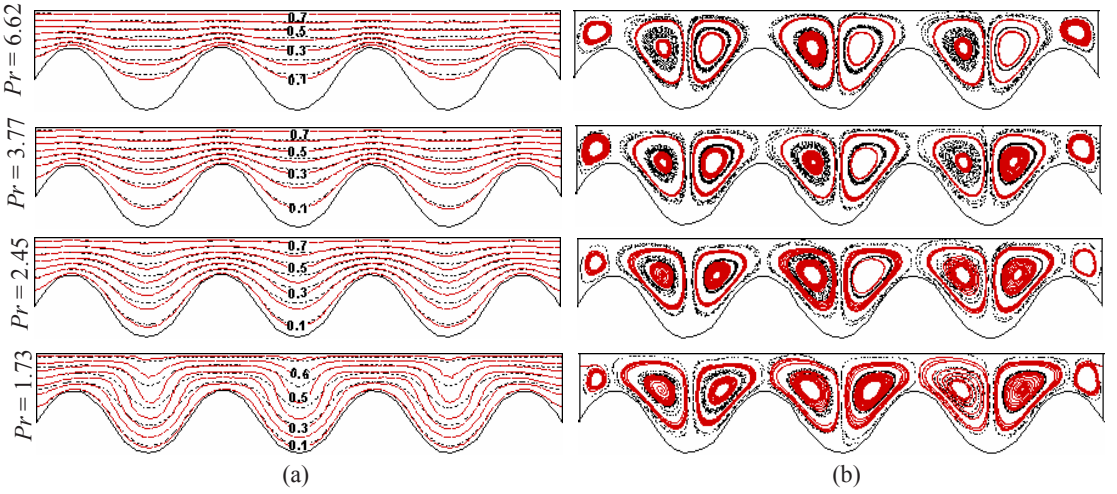

Fig. 5. Effect of Pr on (a) Isotherms and (b) Streamlines at $Ra = 10^4$ (solid lines for nanofluid and dashed lines for base fluid)

Fig. 6(i)-(iii) displays the Nu_c, Nu_r, θ_{av} and ω_{av} for the effect of Prandtl number Pr. Mounting Pr enhances average Nusselt number for both convection and radiation. From Fig. 6 (i), it is found that, rate of convective heat transfer enhances by 26% and 18% for nanofluid and base fluid respectively whereas this rate for radiation is 8% with the increasing values of Pr from 1.73 to 6.62. On the other hand, θ_{av} devalues due to the variation of Pr as temperature of fluid grows down with growing Pr. ω_{av} has notable changes with different values of Prandtl number.

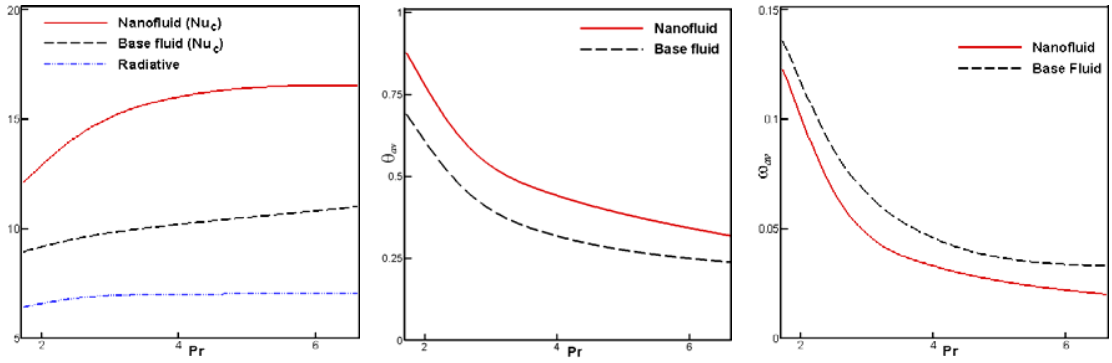

Fig. 6. Effect of *Pr* on (i) *Nu* (ii) θ_{av} and (iii) ω_{av} at $Ra = 10^4$

5. Conclusions

The influence of Prandtl number on natural convection boundary layer flow inside a solar collector with water-Al_2O_3 nanofluid is accounted. Various Prandtl number have been considered for the flow and temperature fields as well as the convective and radiated heat transfer rates, mean bulk temperature of the fluids and average velocity field in the collector while *Ra*, ϕ and ε are fixed at 10^4, 5% and 0.9 respectively. The results of the numerical analysis lead to the following conclusions:

- The structure of the fluid streamlines and isotherms within the solar collector is found to significantly depend upon the *Pr*.
- The Al_2O_3 nanoparticles with the highest *Pr* is established to be most effective in enhancing performance of heat transfer rate than base fluid.
- Average heat transfer is obtained higher for convection than radiation.
- Mean temperature diminishes for both fluids with rising mentioned parameter.
- Average velocity field increases due to falling *Pr*.

Overall the analysis also defines the operating range where water-Al_2O_3 nanofluid can be considered effectively in determining the level of heat transfer augmentation.

Acknowledgement

The work is supported by the department of Mathematics, Bangladesh University of Engineering & Technology.

References

[1] Sukhatme SP. Solar energy, principles of thermal collection and storage. New Delhi, Tata McGraw-Hill, 1991.
[2] Nag A, Misra D, De KE, Bhattacharya A, Saha SK. Parametric study of parallel flow flat plate solar collector using finite element method, In: Numerical Methods in Thermal Problems. Proceedings of the 6th International Conference, Swansea, UK, 1989.
[3] Stasiek JA. Experimental studies of heat transfer and fluid flow across corrugated-undulated heat exchanger surfaces. Int. J. Heat Mass Transfer 1998; 41: 899-914.
[4] Piao Y, Hauptmann EG, Iqbal M. Forced convective heat transfer in cross-corrugated solar air heaters. ASME Journal of Solar Energy Engineering 1994; 116: 212-214.
[5] Gao W. Analysis and performance of a solar air heater with cross corrugated absorber and back-plate. MS thesis, Yunnan Normal University, Kunming, 1996.
[6] Ho CD, Chen TC. The recycle effect on the collector efficiency improvement of double-pass sheet-and-tube solar water heaters with external recycle. Renewable Energy 2006; 31: 953–97.
[7] Hussain A. The performance of a cylindrical solar water heater. Renewable Energy 2006; 31: 1751–1763.
[8] Xiaowu W, Hua B. Energy analysis of domestic-scale solar water heaters. Renewable Sustainable Energy Rev. 2005; 9: 638–645.

[9] Xuesheng W, Ruzhu W, Jingyi W. Experimental investigation of a new-style double-tube heat exchanger for heating crude oil using solar hot water. Appllied Therm. Eng. 2005; 25: 1753–1763.
[10] Hwang Y, Lee JK, Lee CH, Jung YM, Cheong SI, Lee CG, Ku BC, Jang SP. Stability and thermal conductivity characteristics of nanofluids. Thermochimica Acta. 2007; 455: 70–74.
[11] Tripanagnostopoulos Y, Souliotis M, Nousia Th. Solar collectors with colored absorbers. Solar Energy. 2000; 68: 343–356.
[12] Wazwaz J, Salmi H, Hallak R. Solar thermal performance of a nickel-pigmented aluminium oxide selective absorber. Renewable Energy. 2002; 27: 277–292
[13] Orel ZC, Gunde MK, Hutchins MG. Spectrally selective solar absorbers in different non-black colours. Proceedings of WREC VII, Cologne on CD-ROM, 2002.
[14] Konttinen P, Lund PD, Kilpi RJ. Mechanically manufactured selective solar absorber surfaces. Solar Energy Mater Solar Cells. 2003; 79: 273–283.
[15] Lin, KC, Violi, A. Natural convection heat transfer of nanofluids in a vertical cavity: Effects of non-uniform particle diameter and temperature on thermal conductivity. International Journal of Heat and Fluid Flow. 2010; 31: 236–245.
[16] Brinkman, HC. The viscosity of concentrated suspensions and solution. J. Chem. Phys. 1952; 20: 571–581.
[17] Maxwell-Garnett, JC. Colours in metal glasses and in metallic films. Philos. Trans. Roy. Soc. A. 1904; 203: 385–420.
[18] Saleh, H., Roslan, R., Hashim, I. Natural convection heat transfer in a nanofluid-filled trapezoidal enclosure. International Journal of Heat and Mass Transfer. 2011; 54: 194–201.
[19] Taylor, C., Hood, P. A numerical solution of the Navier-Stokes equations using finite element technique. Computer and Fluids. 1973; 1: 73–89.
[20] Dechaumphai, P. Finite Element Method in Engineering, 2nd ed., Chulalongkorn University Press, Bangkok, 1999.
[21] Gao, W., Lin, W., Lu, E. Numerical study on natural convection inside the channel between the flat-plate cover and sine-wave absorber of a cross-corrugated solar air heater. Energy Conversion & Management. 2000; 41: 145-151.